

Supplementary Methods

Chronic Cranial Window Preparation

For chronic window imaging, C57BL/6 mice (20-23g, female, Charles River) underwent surgery when they were ~12-weeks old. This strain was preferred because of their lower propensity to develop neuroinflammation¹, thus allowing for a longer life for chronic imaging. Only females were included because of their calm behavior, easier housing and handling. Also, sex differences would affect stall parameters due to the effect of estrogen and testosterone on vasculature and binding of blood cells to endothelium^{2,3}. Mice were injected with dexamethasone (4.8 mg/kg, i.p.) 4-6 hours before surgery to decrease cerebral edema and inflammation. Under isoflurane, after removal of hair and sterilization of the surgical site, a circular skin incision is made. Exposed periosteum is removed by a #15 blade to ensure good fixation. A custom-made aluminium bar allowing repeated head immobilization was glued to the right side of the skull and a 3x3 mm round craniotomy was performed over the left somatosensory cortex, keeping the dura intact. A plug was prepared by fusion of three 3-mm and one 5-mm diameter cover glasses by an ultraviolet-cured optical adhesive (Norland-61). The plug was inserted into the craniotomy and fixed with dental cement. The bottom surface of the plug was gently touching the brain surface without excessive pressure to prevent compression of the blood vessels. Exposed skull was covered with cement.

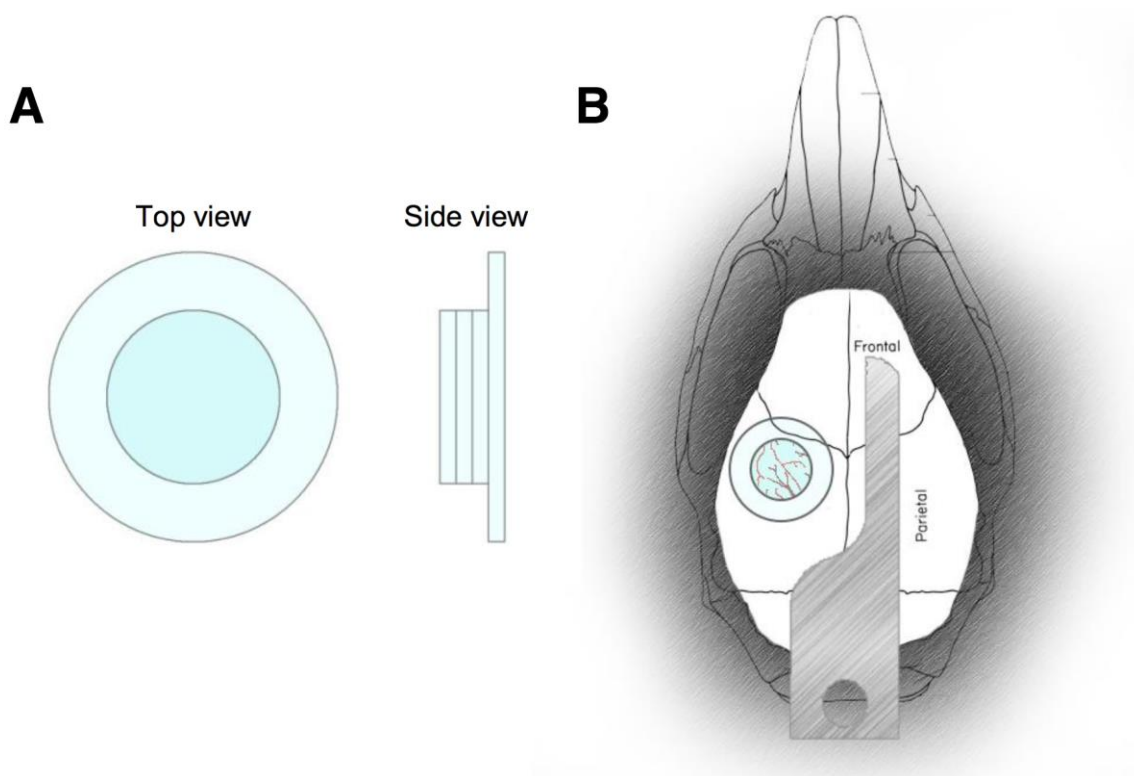


Figure 1. (A) Schematic of the glass plug inserted into the cranial window. (B) Placement of the headpost and cranial window with respect to the anatomical landmarks of the skull.

Mice were then injected with cefazolin (0.5 g/kg, i.p.) and buprenorphine (0.05 mg/kg, s.c.) for infection prophylaxis and analgesia, respectively. Mice were given ibuprofen (20 mg/ml) and trimethoprim-sulfomethoxazole (40/8 mg/ml) in drinking water in addition to cefazolin (0.5 g/kg, i.p., once daily) for 5 days. Mice were then allowed to recover for two weeks after surgery. After this recovery period, an additional 2 weeks were spent for the training of the mice, to tolerate head restraint for the duration of imaging sessions. Mice were attached through their holding bar to the restraint device, in prone position over a suspended bed, with their limbs feely moving. Training durations were gradually increased from 15 min to 2 hours. They were rewarded with sweetened milk as they stayed motionless under restraint. The first imaging sessions were performed when mice were ~4 months old (1 month after cranial

window preparation). During imaging, mice were fixed to the same training cradle and rewarded with milk every 15 minutes.

DLS velocimetry

Dynamic Light Scattering–OCT (DLS-OCT)⁴⁻⁶ was utilized to quantify the blood flow velocity in the stalling and non-stalling capillary segments. DLS-OCT data was acquired using an M-mode scanning pattern (i.e. repeat A-scans for each (x,y) position), and was performed in the same ROI as the OCT-angiogram. We performed 100 repeated A-scans for each spatial position (x,y) to calculate the autocorrelation function with 25 time-lag points. The acquisition time for 100 A-scans was ~2.2 ms which was short enough to avoid motion artifacts primarily resulting from cardiac pulsation (71-194 ms⁷) and respiration (261-750 ms⁸). Total time to acquire one volume of DLS-OCT data was ~6.5 min.

Offline data processing was performed with MATLAB on a 200-core cluster system provided by the Martinos Center for Biomedical Imaging. Data spanning 150-250 μm beneath the brain surface (same depth range as the OCT-angiogram) was extracted from each A-line. Experimental electric field temporal autocorrelation functions (g_{1exp}) were calculated for each voxel (x,y,z). Then, M_S , M_F , v_t , v_z , and D were obtained for each voxel (x,y,z) by fitting the theoretical electric field autocorrelation function $g_1(\tau)$ given by **Equation (1)**⁴ to the measured $g_{1exp}(\tau)$.

$$g_1(\tau) = E \left[\frac{\langle R_1^*(t)R_1(t+\tau) \rangle_t}{\langle R_1^*(t)R_1(t) \rangle_t} \right] = M_S + M_F e^{-h_t^2 v_t^2 \tau^2 - h^2 v_z^2 \tau^2} \cdot e^{-q^2 D \tau} \cdot e^{iq v_z \tau} + M_E \delta(\tau) \quad (1)$$

where, M_S is the composition ratio of static particles; M_F and $M_E = (1 - M_S - M_F)$ is the composition ratio of flowing/ diffusing particles and entering/exiting particles, respectively; v_t is the transverse component of the flow velocity, v_z is the axial component of the flow velocity, and D is the diffusion coefficient, $h=0.5 \mu m^{-1}$ is the inverse of the 1/e width of axial resolution, and $h_t = 0.5 \mu m^{-1}$ is the inverse of the 1/e width of tranverse resolution when using the 10X objective.

Whisker Stimulation Experiments

Experiments were performed in awake animals (n=6), as they were fixed to the imaging cradle. Laser speckle contrast imaging (LSCI) was performed as described previously^{9, 10} to monitor functional hyperemia. Briefly, the left-sided cranial window was illuminated with a 915 nm laser diode (Thorlabs). Raw speckle images (~2.2x1.8 mm area) were acquired using a CCD camera (Basler acA1300-200am) connected to the OCT imaging microscope with a dichroic mirror. Sixty raw images were acquired every 0.5 seconds, converted to speckle contrast images and averaged online using a custom software (kindly provided by Andrew Dunn, University of Texas in Austin). Speckle contrast values were converted to correlation-time values, then relative blood flow images (showing the % change in blood flow compared to baseline) were also generated by dividing the correlation-time values of each pixel at any time by the baseline value. After a preliminary run to identify the activation center in relative blood flow maps, OCT imaging was directed into this ROI. OCT angiograms (120 frames in total) were acquired simultaneously with LSCI during baseline, during stimulation and resting periods. After 15 baseline OCT angiograms, whiskers were stimulated during 16-20th, 31-35th, 46-50th, 61-65th, 76-80th and 91-95th frames, with a cotton tip applicator in dorsoventral direction (5-8 Hz for 45 seconds). No external whisker stimulation was applied during the resting intervals. Functional activation was confirmed by checking the LSCI relative blood flow images during each activation. All stimulation trials resulted in a hyperemic response in the cortex. During analysis, the data was divided into pre-stimulation, stimulation and post-stimulation epochs, each consisting of 5 consecutive OCT angiogram frames. Stall incidence (percentage of segments that stalled any time during the epoch over all segments) and point prevalence (percentage of stalled segments at each time point) were calculated and averaged across the same-type-epochs of the experiment. In the control group, the same animals for

whisker stimulation were imaged at a different day, with the identical imaging protocol, but without external whisker stimulation. The OCT data was divided into the same epochs with the simulation group, with respect to the frame numbers.

Two-Photon microscopy (TPM) imaging

A commercial TPM system (Ultima, Prairie Technologies) was used with a 20X water-immersion objective (Olympus XLumPlan Fluor, 1.00 NA, 2-mm working distance). For visualization of the vasculature, 0.2 ml Rhodamine B-Dextran (70KDa) was retroorbitally injected 30-min before imaging. The dye was excited at 840nm using a tunable, pulsed Titanium:Sapphire laser (100fs pulse duration, 80MHz repetition rate, Mai-Tai Tsunami, Spectra-Physics) and scanned across the field of view using galvanometer scanning mirrors. Using dichroic beam splitters and optical bandpass filters, the emitted fluorescence light was collected through the objective and directed to photomultiplier tube detectors (525 ± 25 nm). TPM scanning was done under awake, resting conditions. Z-stacks (2- μ m slice interval) of each ROI (~600x600 μ m) were acquired at 1.136 μ m/pixel resolution. MIP images of the TPM angiograms were manually registered to the OCT-angiograms. In TPM angiograms, stalling and nonstalling capillaries were traced to the nearest penetrating arteriole/venule and their branching orders were determined. Capillary-size vessels (diameter <10 μ m) branching directly from the penetrating vessels were coded as A1 or V1, for upstream (arteriole) and downstream (venule) sides respectively. If a vessel with a larger diameter was branching from the penetrating vessel, then the first subsequent branch with a capillary size was coded as A1/V1. For 3D-visualizations of selected capillaries, and calculations of segment lengths and tortuosity indices (total segment length divided by the Euclidian distance between the segment lengths¹¹), FIJI with the Simple Neurite Tracer Plug-In was used¹².

References

1. Nikodemova M, Watters JJ. Outbred ICR/CD1 mice display more severe neuroinflammation mediated by microglial TLR4/CD14 activation than inbred C57Bl/6 mice. *Neuroscience* 2011; 190: 67-74.
2. Cid MC, Kleinman HK, Grant DS, Schnaper HW, Fauci AS, Hoffman GS. Estradiol enhances leukocyte binding to tumor necrosis factor (TNF)-stimulated endothelial cells via an increase in TNF-induced adhesion molecules E-selectin, intercellular adhesion molecule type 1, and vascular cell adhesion molecule type 1. *J Clin Invest* 1994; 93(1): 17-25.
3. Kelly DM, Jones TH. Testosterone: a vascular hormone in health and disease. *J Endocrinol* 2013; 217(3): R47-71.
4. Lee J, Wu W, Jiang JY, Zhu B, Boas DA. Dynamic light scattering optical coherence tomography. *Optics express* 2012; 20(20): 22262-22277.
5. Lee J, Radhakrishnan H, Wu W, Daneshmand A, Climov M, Ayata C *et al.* Quantitative imaging of cerebral blood flow velocity and intracellular motility using dynamic light scattering–optical coherence tomography. *Journal of Cerebral Blood Flow & Metabolism* 2013; 33(6): 819-825.
6. Tang J, Erdener SE, Fu B, Boas DA. Capillary red blood cell velocimetry by phase-resolved optical coherence tomography. *Opt Lett* 2017; 42(19): 3976-3979.
7. Ho D, Zhao X, Gao S, Hong C, Vatner DE, Vatner SF. Heart rate and electrocardiography monitoring in mice. *Current protocols in mouse biology* 2011: 123-139.
8. Zehendner CM, Luhmann HJ, Yang J-W. A simple and novel method to monitor breathing and heart rate in awake and urethane-anesthetized newborn rodents. *PLoS one* 2013; 8(5): e62628.
9. Dunn AK, Devor A, Bolay H, Andermann ML, Moskowitz MA, Dale AM *et al.* Simultaneous imaging of total cerebral hemoglobin concentration, oxygenation, and blood flow during functional activation. *Opt Lett* 2003; 28(1): 28-30.
10. Dunn AK, Bolay H, Moskowitz MA, Boas DA. Dynamic imaging of cerebral blood flow using laser speckle. *J Cereb Blood Flow Metab* 2001; 21(3): 195-201.
11. Helmberger M, Pienn M, Urschler M, Kullnig P, Stollberger R, Kovacs G *et al.* Quantification of tortuosity and fractal dimension of the lung vessels in pulmonary hypertension patients. *PLoS One* 2014; 9(1): e87515.

12. Longair MH, Baker DA, Armstrong JD. Simple Neurite Tracer: open source software for reconstruction, visualization and analysis of neuronal processes. *Bioinformatics* 2011; 27(17): 2453-4.